Electrocatalysis

DOI: 10.1002/ange.201308620

An Effective Pd–Ni_2P/C Anode Catalyst for Direct Formic Acid Fuel Cells**

Jinfa Chang, Ligang Feng, Changpeng Liu, Wei Xing, and Xile Hu**

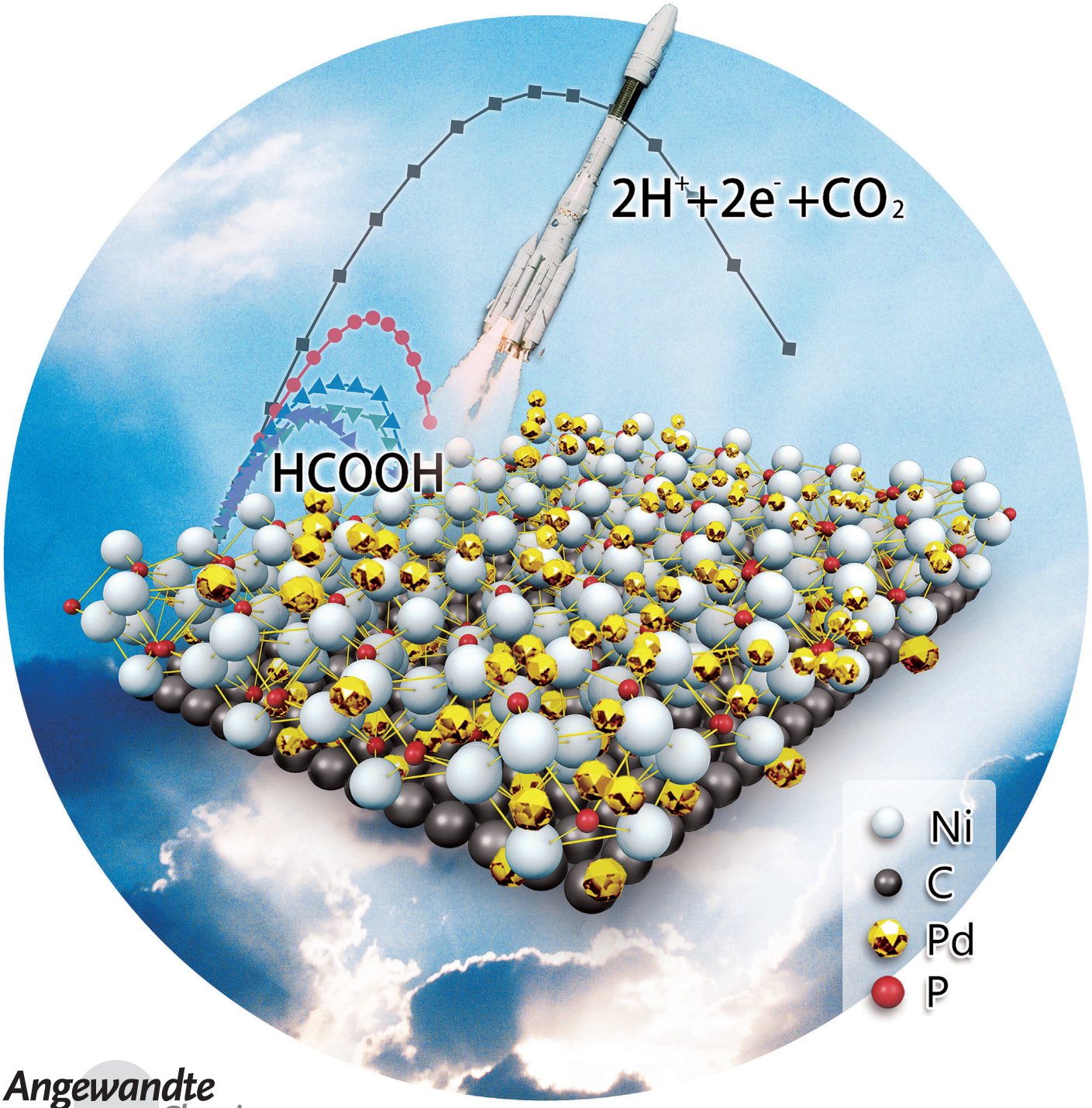

Abstract: *The direct formic acid fuel cell is an emerging energy conversion device for which palladium is considered as the state-of-the-art anode catalyst. In this communication, we show that the activity and stability of palladium for formic acid oxidation can be significantly enhanced using nickel phosphide (Ni_2P) nanoparticles as a cocatalyst. X-ray photoelectron spectroscopy (XPS) reveals a strong electronic interaction between Ni_2P and Pd. A direct formic acid fuel cell incorporating the best Pd–Ni_2P anode catalyst exhibits a power density of 550 mW cm^{-2}, which is 3.5 times of that of an analogous device using a commercial Pd anode catalyst.*

Direct formic acid fuel cells are considered to be a promising power source for portable electronic devices. The development of active anode catalysts for the oxidation of formic acid is therefore an active area of research.[1] Pd-based catalysts have recently drawn attention because they can catalyze the oxidation of formic acid by a direct path that reduces the poisoning effect associated with conventional Pt catalysts.[2] Increasing the activity of Pd can lead to a lower usage of this rare and costly metal. Several nanostructured Pd catalysts exhibited a high performance for formic acid oxidation; however, these catalysts were synthesized under harsh conditions and required cumbersome post-treatments.[2b,3] The addition of Ni, Co, Fe, P, or N is reported to enhance the catalytic activity of Pd.[4] Unfortunately, the dissolution or instability of the promoter elements results in the rapid decay of catalytic performance.

Herein, we demonstrate that Ni_2P can act as a stable cocatalyst for Pd-catalyzed formic acid oxidation. The Pd–Ni_2P/C anode system shows remarkable catalytic activity and stability. When integrated in a direct formic acid fuel cell, the hybrid catalyst gives power density and discharge stability superior to several state-of-the-art catalysts.

The Ni_2P/C particles were synthesized by a solid phase reaction. Pd was deposited onto Ni_2P/C by a microwave-assisted ethylene glycol reduction method (see the Supporting Information for details). The Raman spectra of Ni_2P/C particles display two very distinctive D and G bands at 1331 and 1589 cm^{-1}, respectively (Supporting Information, Figure S1). The D band arises from structural defects in the graphitic plane, whereas the G band is related to the E_{2g} vibrational mode of the sp^2-bonded graphitic carbons. In the XRD pattern of the Ni_2P/C, the diffraction peaks of Ni_2P are visible (Figure S2). These peaks are not observed in the XRD pattern of Pd–Ni_2P/C; however, the presence of Ni_2P was confirmed by EDS (Figure S3 g) and element distribution maps (Figure S3 a–f). Typical TEM images of Ni_2P/C and Pd–Ni_2P/C (30 wt % of Ni_2P on C) are shown in Figure 1. The

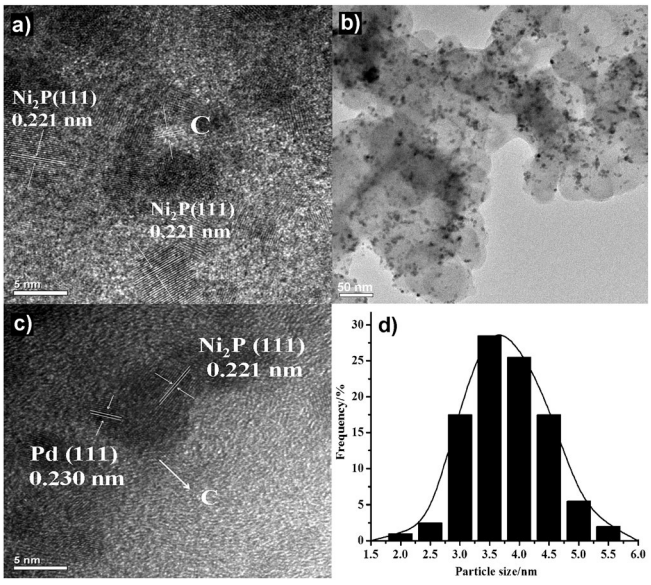

Figure 1. a) HRTEM image of Ni_2P/C where the (111) lattice of Ni_2P can be observed, and the carbon support is visible. b) TEM image of the Pd–Ni_2P/C catalyst. c) HRTEM image of Pd–Ni_2P/C catalyst; both Pd(111) and Ni_2P(111) lattices can be observed, and the carbon support is visible. d) Size distribution of the Pd–Ni_2P/C catalyst. Scale bars in (a) and (c) are 5 mm, scale bar in (b) is 50 nm.

Ni_2P nanoparticles can be observed with a finger lattice of 0.221 nm, which corresponds to its (111) lattice (Figure 1 a).[5] After deposition of Pd, the Pd nanoparticles were uniformly distributed on the Ni_2P/C hybrid support with a narrow size distribution; the average particle size of Pd is about 3.5 nm (Figure 1 b,d), which is an optimal particle size for formic acid oxidation.[1g,2e,6] Finger lattices of Ni_2P and Pd can both be observed (Figure 1 c). The particle size of Pd in other samples where the wt % of Ni_2P on C varied was also about 3.5 nm (Figure S4).

Typical Pd electrochemical behaviors for all Pd–Ni_2P/C samples were observed in H_2SO_4 (0.5 M; Figure S5). The Pd–Ni_2P/C (30 wt % of Ni_2P on C) catalyst shows the largest electrochemical surface area (ECSA), according to the area of the hydrogen desorption peaks (Table S1). The more accurate ECSA obtained from CO-stripping experiments (Figure S6) were used to calculate the specific activity for all catalysts. The peak potential of the adsorbed CO is commonly

[*] J. F. Chang,[+] Prof. Dr. C. Liu, Prof. Dr. W. Xing
State Key Laboratory of Electroanalytical Chemistry, Laboratory of Advanced Power Sources, Changchun Institute of Applied Chemistry, Chinese Academy of Sciences, Changchun 130022 (P.R. China)
E-mail: xingwei@ciac.jl.cn
Dr. L. G. Feng,[+] Prof. Dr. X. L. Hu
Institute of Chemical Sciences and Engineering, Ecole Polytechnique Fédérale de Lausanne (EPFL)
ISIC-LSCI, BCH 3305, Lausanne 1015 (Switzerland)
E-mail: xile.hu@epfl.ch
Homepage: http://lsci.epfl.ch
[+] These authors contributed equally to this work.

[**] The work in CAS is supported by the National Basic Research Program of China (973 Program, 2012CB215500, 2012CB932800), the National High Technology Research and Development Program of China (863 Program, 2012AA053401), the Recruitment Program of Foreign Experts (WQ20122200077), the National Natural Science Foundation of China (20933004, 21073180) and the Strategic priority research program of CAS (XDA0903104). The work at EPFL is supported by a grant from the Competence Center for Energy and Mobility (CCEM) in the framework of the Hytech project.
Supporting information for this article is available on the WWW under http://dx.doi.org/10.1002/anie.201308620.

used as a tool to compare the antipoisoning ability.[1b,e] The Pd–Ni_2P/C (30 wt % Ni_2P) catalyst has the most negative peak potential (Table S1), thus indicating that this material has the best anti-poisoning ability.

The activities of Pd–Ni_2P/C catalysts with different weight percentages of Ni_2P were compared (see Figure 2 for mass

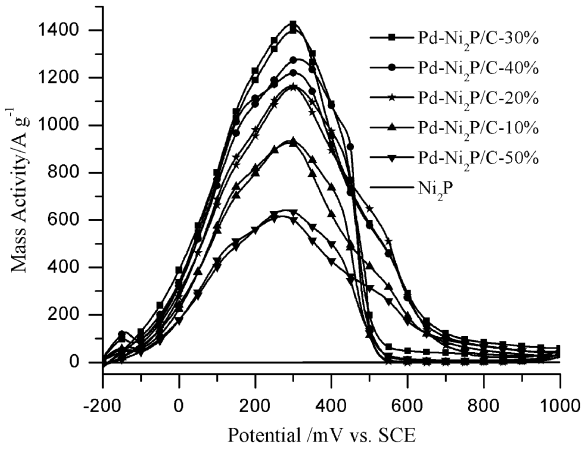

Figure 2. Cyclic voltammograms of Ni_2P and Pd–Ni_2P with different amounts of Ni_2P in H_2SO_4 solution (0.5 M) containing HCOOH (0.5 M) at 50 $mV s^{-1}$.

activity; see also Figure S7 for specific activity and Table S2 for an overall comparison). Ni_2P alone has almost no catalytic activity, but it has a strong influence on the activity of Pd. The optimized loading is 30 % Ni_2P on C. The Pd–Ni_2P/C-30 % catalyst has the best catalytic stability, based on chronoamperometric (CA) measurements (Figure S8). Electrochemical impedance spectroscopy (EIS) and X-ray photoelectron spectroscopy (XPS) were applied to investigate the influence of Ni_2P loading. Based on EIS analysis (Figure S9), it was hypothesized that more formic acid is oxidized around the peak potential of the Pd–Ni_2P/C-30 % catalyst, probably owing to reduced passivation at Pd. In the XPS spectra, a shift in the Pd binding energy was observed (see below); this shift was the same in all samples, regardless of Ni_2P loading (Figure S10). Thus, the optimal loading of Ni_2P likely arises from a balanced interaction between Pd and Ni_2P, rather than simply from an optimal electronic effect, which would have been detected by XPS.

The Pd–Ni_2P/C-30 % catalyst was compared with the state-of-the-art commercial Pd/C (Pd/C–C) catalyst, home-made Pd/C (Pd/C–H), PdNi/C and PdP/C catalysts by linear sweep voltammetry (see Figure 3 for mass activity; see also Figure S11 for specific activity). Among all these catalysts, Pd–Ni_2P/C-30 % exhibits the best activity for formic acid oxidation. PdP/C and PdNi/C performed slightly better than Pd/C–H, but are largely inferior to Pd–Ni_2P/C. The promotional effect of the Ni_2P is therefore much larger than P or Ni alone. The Tafel slopes of these catalysts were also compared (Figure S12), and Pd–Ni_2P/C-30 % has the smallest Tafle slope (Table S3), which is advantageous for practical applications. Furthermore, the specific activity of Pd–Ni_2P/C-30 % compares favorably with other recently reported catalysts

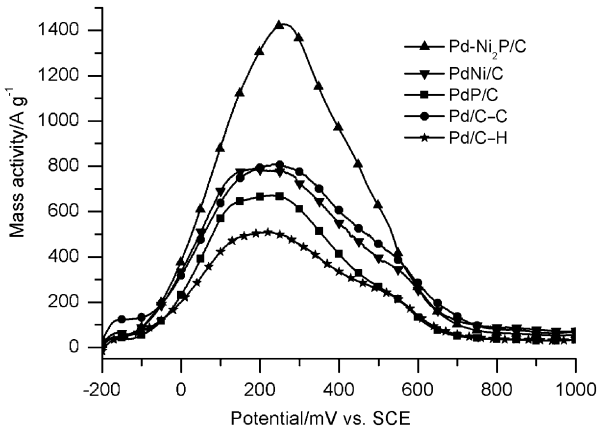

Figure 3. Linear sweep voltammograms of Pd–Ni_2P-30 %, PdNi/C, PdP/C, Pd/C–C and Pd/C–H in H_2SO_4 solution (0.5 M) containing HCOOH (0.5 M) at 50 $mV s^{-1}$.

(Table S4). The stability of catalysts was probed by chronoamperometric measurements with stationary and rotating disk electrodes (Figure S13). The Pd–Ni_2P/C-30 % catalyst exhibits the best stability for formic acid oxidation, with the highest stable currents.

XPS was applied to probe the origin of the promotional effect of Ni_2P. From Pd to Pd–Ni_2P/C (Figure 4), the Pd 3d peaks are shifted significantly, by about 1 eV, to a lower binding energy. This shift might be attributed to an partial electron transfer from Ni_2P to Pd; this would increase the electron density of Pd and enhance the penetration of outer-layer electrons to the inner layer.[7] This results in higher shielding of the nuclear charge and weakens the binding of 3d electrons. On the other hand, the Pd 3d peaks are not substantially shifted from Pd to PdNi/C and PdP/C. These results suggest that the enhanced activity and stability of Pd–Ni_2P/C might be attributed to a strong electronic interaction between Pd and Ni_2P. In addition to the electronic effect, Ni_2P might directly participate in formic acid oxidation. Recently, Ni_2P was found to be an effective hydrogen evolution catalyst.[8] Hydrogen adsorption might be facile on Ni_2P,

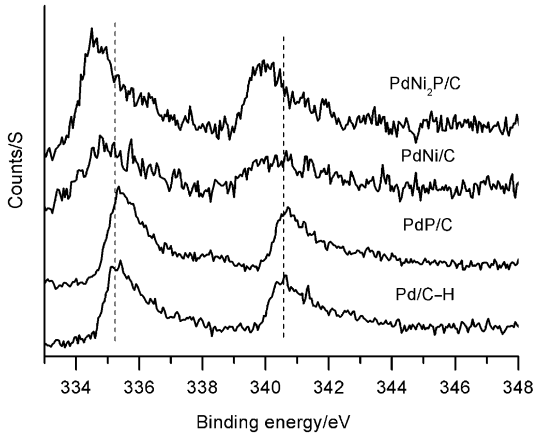

Figure 4. XPS spectra of the Pd 3d region for Pd–Ni_2P/C-30 %, PdNi/C, PdP/C, and Pd/C–H.

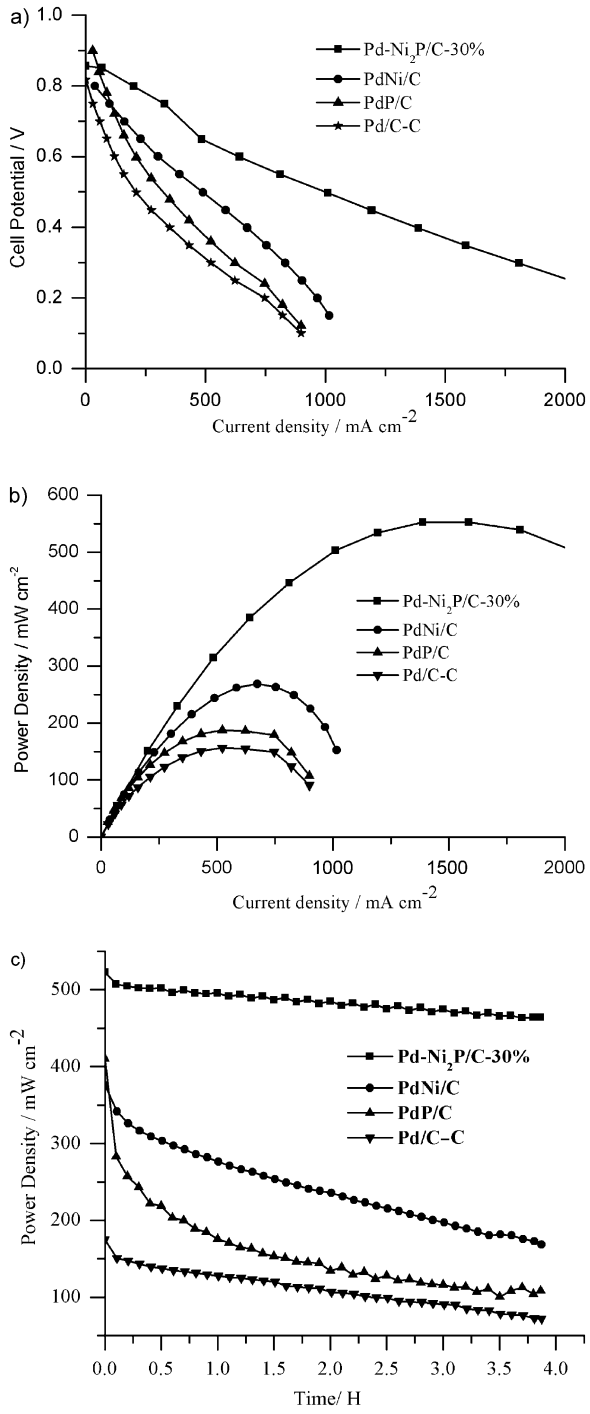

Figure 5. a) Steady-state polarization, b) power-density curves and c) discharge curves at 0.35 V for Pd–Ni_2P/C-30%, PdNi/C, PdP/C and Pd/C–C as anode catalysts for the direct formic acid fuel cell with formic acid (3 M) at 30 °C. The flow rate of formic acid was 200 mL min^{-1} and the flow rate of O_2 was 500 mL min^{-1}.

which might accelerate formic acid oxidation in a fashion similar to the hydrogen spill-over effect.[9] Ni_2P might also activate water, producing -OH_{ads} to oxidize CO and other poisoning intermediates adsorbed at adjacent Pd sites through the so-called bifunctional mechanism.[1a,g] More work is required to test these mechanistic hypotheses.

To demonstrate the potential of the Pd–Ni_2P/C catalyst in a direct formic acid fuel cell, the catalyst was integrated at the anode of a homemade fuel cell. The steady-state polarization and power-density curves of several catalysts were compared (Figure 5a,b). Consistent with the results from electrochemical measurements, the Pd–Ni_2P/C-30% catalyst exhibits the highest power density. This power density of 550 mW cm^{-2} is about 2 times of that of PdNi/C, 3 times of that of PdP/C, and 3.5 times of that of a state-of-the-art Pd/C commercial catalyst. Moreover, the Pd–Ni_2P/C catalyst also shows the most stable discharge ability at 0.35 V (Figure 5c). These results confirm the promising activity of Pd–Ni_2P/C for direct formic acid fuel cell.

In summary, a novel Pd–Ni_2P/C electrocatalyst was developed for formic acid oxidation. The catalyst exhibited excellent activity and stability, and was successfully integrated into a direct formic acid fuel cell, showing superior performance to a state-of-the-art Pd/C catalyst. The work is a significant step towards the development of more active and practical catalysts for direct formic acid fuel cells.

Received: October 3, 2013
Published online: November 25, 2013

Keywords: electrocatalysis · formic acid · fuel cells · oxidation · nickel

[1] a) Y. X. Chen, M. Heinen, Z. Jusys, R. J. Behm, *Angew. Chem.* **2006**, *118*, 995 – 1000; *Angew. Chem. Int. Ed.* **2006**, *45*, 981 – 985; b) W. Gao, J. E. Mueller, Q. Jiang, T. Jacob, *Angew. Chem.* **2012**, *124*, 9584 – 9589; *Angew. Chem. Int. Ed.* **2012**, *51*, 9448 – 9452; c) F. J. Vidal-Iglesias, A. López-Cudero, J. Solla-Gullón, J. M. Feliu, *Angew. Chem.* **2012**, *124*, 1 – 1; *Angew. Chem. Int. Ed.* **2012**, *51*, 1 – 5; d) F. J. Vidal-Iglesias, J. Solla-Gullón, E. Herrero, A. Aldaz, J. M. Feliu, *Angew. Chem.* **2010**, *122*, 7152 – 7155; *Angew. Chem. Int. Ed.* **2010**, *49*, 6998 – 7001; e) S. Zhang, Y. Shao, G. Yin, Y. Lin, *Angew. Chem.* **2010**, *122*, 2257 – 2260; *Angew. Chem. Int. Ed.* **2010**, *49*, 2211 – 2214; f) D. Chen, Z. Zhou, Q. Wang, D. Xiang, N. Tian, S. Sun, *Chem. Commun.* **2010**, *46*, 4252 – 4254; g) L. Feng, X. Sun, C. Liu, W. Xing, *Chem. Commun.* **2012**, *48*, 419 – 421; h) M. K. Debe, *Nature* **2012**, *486*, 43 – 51; i) R. F. Service, *Science* **2002**, *296*, 1222 – 1224.

[2] a) H. Lee, S. E. Habas, G. A. Somorjai, P. Yang, *J. Am. Chem. Soc.* **2008**, *130*, 5406 – 5407; b) V. Mazumder, S. Sun, *J. Am. Chem. Soc.* **2009**, *131*, 4588 – 4589; c) Z. Bai, L. Yang, Y. Guo, Z. Zheng, C. Hu, P. Xu, *Chem. Commun.* **2011**, *47*, 1752 – 1754; d) S. Patra, B. Viswanath, K. Barai, N. Ravishankar, N. Munichandraiah, *ACS Appl. Mater. Interfaces* **2010**, *2*, 2965 – 2969; e) E. Antolini, *Energy Environ. Sci.* **2009**, *2*, 915 – 931.

[3] a) X. X. Wang, J. D. Yang, H. J. Yin, R. Song, Z. Y. Tang, *Adv. Mater.* **2013**, *25*, 2728 – 2732; b) V. Mazumder, M. F. Chi, M. N. Mankin, Y. Liu, O. Metin, D. H. Sun, K. L. More, S. H. Sun, *Nano Lett.* **2012**, *12*, 1102 – 1106; c) C. Liao, Z. D. Wei, S. G. Chen, L. Li, M. B. Ji, Y. Tan, M. J. Liao, *J. Phys. Chem. C* **2009**, *113*, 5705 – 5710.

[4] a) C. Du, M. Chen, W. Wang, G. Yin, *ACS Appl. Mater. Interfaces* **2010**, *2*, 105 – 109; b) C. Du, M. Chen, W. Wang, G. Yin, P. Shi, *Electrochem. Commun.* **2010**, *12*, 843 – 846; c) X. M. Wang, Y. Y. Xia, *Electrochem. Commun.* **2008**, *10*, 1644 – 1646; d) L. L. Zhang, Y. W. Tang, J. C. Bao, T. H. Lu, C. Li, *J. Power Sources* **2006**, *162*, 177 – 179; e) J. Jia, R. Wang, H. Wang, S. Ji, J. Key, V. Linkov, K. Shi, Z. Lei, *Catal. Commun.* **2011**, *16*, 60 – 63; f) B. M. Leonard, Q. Zhou, D. Wu, F. J. DiSalvo, *Chem. Mater.* **2011**, *23*, 1136 – 1146;

g) G. Yang, Y. Chen, Y. Zhou, Y. Tang, T. Lu, *Electrochem. Commun.* **2010**, *12*, 492 – 495.
[5] Y. Lu, X. L. Wang, Y. J. Mai, J. Y. Xiang, H. Zhang, L. Li, C. D. Gu, J. P. Tu, S. X. Mao, *J. Phys. Chem. C* **2012**, *116*, 22217 – 22225.
[6] a) L. L. Zhang, T. H. Lu, J. C. Bao, Y. W. Tang, C. Li, *Electrochem. Commun.* **2006**, *8*, 1625 – 1627; b) N. Cheng, R. A. Webster, M. Pan, S. Mu, L. Rassaei, S. C. Tsang, F. Marken, *Electrochim. Acta* **2010**, *55*, 6601 – 6610.
[7] D. J. Ham, C. Pak, G. H. Bae, S. Han, K. Kwon, S.-A. Jin, H. Chang, S. H. Choi, J. S. Lee, *Chem. Commun.* **2011**, *47*, 5792 – 5794.
[8] E. J. Popczun, J. R. McKone, C. G. Read, A. J. Biacchi, A. M. Wiltrout, N. S. Lewis, R. E. Schaak, *J. Am. Chem. Soc.* **2013**, *135*, 9267 – 9270.
[9] a) K. W. Park, K. S. Ahn, Y. C. Nah, J. H. Choi, Y. E. Sung, *J. Phys. Chem. B* **2003**, *107*, 4352 – 4355; b) L. Feng, Z. Cui, L. Yan, W. Xing, C. Liu, *Electrochim. Acta* **2011**, *56*, 2051 – 2056.